Developmental and Comparative Immunology 34 (2010) 659–668

Contents lists available at ScienceDirect

Developmental and Comparative Immunology

journal homepage: www.elsevier.com/locate/dci

Identification and characterization of the parasitic wasp *Nasonia* defensins: Positive selection targeting the functional region?

Bin Gao, Shunyi Zhu *

Group of Animal Innate Immunity, State Key Laboratory of Integrated Management of Pest Insects & Rodents, Institute of Zoology, Chinese Academy of Sciences, Beijing 100101, China

ARTICLE INFO

Article history:
Received 22 December 2009
Received in revised form 17 January 2010
Accepted 18 January 2010
Available online 2 February 2010

Keywords:
Parasitoid
Recombinant peptide
Innate immunity
Adaptive evolution

ABSTRACT

Defensin is a crucial component of innate immunity highly conserved across different insect orders. Here, we report identification and characterization of defensins in the parasitic wasp *Nasonia* (Hymenoptera: Pteromalidae). In comparison with those in the non-parasitic insect *Apis mellifera*, two different subtypes of defensins (defensin1 and defensin2) have undergone independent gene duplication to create a mutigene family of five members (named 1-1, 1-2, 2-1, 2-2 and 2-3) in the *Nasonia* lineage. Such duplication occurred before the divergence of three sibling species (*N. vitripennis*, *N. giraulti* and *N. longicornis*) and the duplicated genes was subsequently subjected to positive selection at the amino-terminal loop and the γ-core region. RT-PCR identified that only the subtype 1 of defensins were constitutively expressed in the *N. vitripennis* adult stage and none of the five defensins was expressed in other developmental stages (i.e. the infected *Musca domestica* pupae). A functional form of 2-2 in *N. vitripennis* (named navidefensin2-2) was produced in *Escherichia coli* by an on-column refolding approach. The recombinant peptide presented a typical defensin structure, as identified by CD analysis, and selectively inhibited the growth of two Gram$^+$ bacteria at low micromolar concentrations. The bioactive surface responsible for antibacterial activity of navidefensin2-2 was identified in the γ-core region of this molecule. Positive selection targeting the antibacterial region of defensins could be a consequence of evolutionary arms race between *Nasonia* and its pathogens.

1. Introduction

Defensins from non-vertebrate species are among the most extensively distributed antimicrobial peptides (AMPs) found in all three eukaryotic kingdoms. They represent a large family of evolutionarily related cationic effector molecules against microbial infection [1–3]. Despite extensive sequence diversity, the defensins possess a conserved cysteine-stabilized α/β (CSαβ) structure that includes one α-helix and one β-sheet of two antiparallel strands. The α-helix spanning the CXXXC sequence (X, any amino acid) is connected to the second β-strand containing the CXC sequence via two disulfide bridges [4]. A similar structural motif was also found in an antiparasitic defensin-like peptide (AdDLP) from a myxobacterium, suggesting that the ancestor of these defense molecules could have originated in prokaryotes [5]. Interestingly, the structural motif of defensins comprising the two β-strands linked by a turn also exist in many AMPs with different structural types, which has now been called γ-core [6,7].

There are two main classes of defensins in insects, which constitute an essential component of their innate immunity: classical insect-type defensins (CITDs) and ancient invertebrate-type defensins (AITDs), which are easily recognized from their amino acid sequences. CITDs were only found in the orders of modern insects [8] whereas AITDs have a wider phylogenetic distribution. In addition to the presence in some ancient amphibious insects in the order Odonata [9], AITDs are distributed in fungi, mussels, oysters, ticks and scorpions [10–15]. In scorpion venom, some AITDs extended their N-termini into a distinct α-helical domain [16]. Despite low amino acid sequence identity, their co-existence in the same fungal species supports a paralogous relationship between AITDs and CITDs [15].

Different from amphipathic, cationic α-helical AMPs which are active on many different microbes such as bacteria, fungi, yeasts and viruses [17,18], the majority of insect defensins target a broad spectrum of Gram$^+$ bacteria [1]. They rapidly kill bacteria by destroying the cytoplasmic membrane at micromolar concentrations. The protective role of these molecules to the Gram$^+$ bacterial infection has been well documented by *in vivo* targeted disruption of the mosquito *Anopheles gambiae* defensin gene causing the

Abbreviations: 3D, three-dimensional; AMP, antimicrobial peptide; C/EBPα, CCAAT/enhancer binding protein-α; C_L, lethal concentration; CSαβ, cysteine-stabilized α/β motif; EK, enterokinase; HLD, hymenoptaecin-like domain; NFkB, nuclear factor kB; PC, proprotein convertase; PP, propeptide; RT, retention time; SP1, specificity protein1; TFE, trifluoroethanol; TSS, transcriptional start site; TF, transcriptional factor.

* Corresponding author. Fax: +86 10 64807099.
E-mail address: Zhusy@ioz.ac.cn (S. Zhu).

0145-305X/$ – see front matter © 2010 Elsevier Ltd. All rights reserved.
doi:10.1016/j.dci.2010.01.012

death of the mosquitoes after bacterial infection [19]. Some *A. gambiae* defensins are being used as templates for rational design of engineering peptides active against the Gram$^+$ bacteria *Staphylococcus aureus* [20].

Since the first insect defensins were isolated from cell cultures of the flesh fly and experimentally injured larvae of the black blowfly [21,22], numerous insect defensins have been identified in diverse insect species, such as phormicins, sapecins and spodoptericins [23,24]. The parasitic hymenoptera is an ecologically and economically important insect group because many insects in this order are natural enemies of a broad range of arthropods (e.g. pest insects). However, their innate immune system is less known. As the first parasitic hymenopteran insect with its genome sequenced [25], *Nasonia* provides a new resource for the identification of such molecules in this class of insects. Our work presented here represents the first report which describes the genomic identification and characterization of insect defensins from three sibling *Nasonia* species (*N. vitripennis*, *N. giraulti* and *N. longicornis*). By using codon-subsitution models, we detected the positive selection signal in the *Nasonia* defensin family. We recombinantly produced a highly pure *Nasonia* defensin (herein named navidefensin2-2) and identified its biological function and structural feature.

2. Materials and methods

2.1. Gene discovery and database search

Nasonia defensins were found by searching the GenBank genomic database (*N. vitripennis*, *N. giraulti* and *N. longicornis*) (http://www.ncbi.nlm.nih.gov) using TBLASTN program and *Apis mellifera* defensins (Amdefensin-1 and 2) as queries. Signal sequence and propeptide cleavage sites of protein precursors were predicted by ProP 1.0 (http://www.cbs.dtu.dk/services/ProP/).

2.2. Detection of developmental stage-specific expression of defensins

The *N. vitripennis* defensin family member-specific nucleotide sequences were selected for primer design to distinguishably amplify their corresponding cDNAs (Table S1, provided as Supplementary material). To prepare total RNAs of *N. vitripennis*, each 50 mg of 3-day-old adults and the *M. domestica* pupae infected by *N. vitripennis* were separately collected and grounded into fine powder in liquid nitrogen. The total RNAs of these two samples were prepared using TRIZOL reagent (SBS Genetech, Beijing) and were reverse transcribed into first-strand cDNAs using EasyScript First-Strand cDNA Synthesis Kit (TransGen, Beijing) by a universal oligo (dT)-containing adaptor primer (dT3AP). cDNAs of defensins were amplified using specific primers combined with 3AP [26] (Table S1) and their sequences were determined according to the methods described previously. Nucleotide sequences of navidefensin1-1, and 1-2 cDNAs have been deposited in the GenBank database under the accession number of GQ924584 and GQ924585.

2.3. Gene synthesis and expression vector construction

The mature navidefensin2-2 nucleotide sequence was synthesized by Beijing BIOMED TECH (BIOMED, Beijing), in which 6 rare codons in *Escherichia coli* were optimized to improve the expression of navidefensin2-2. The nucleotide sequence has been deposited in the GenBank database under the accession number of GQ463146. The synthesized gene was inserted into pET-28a at BamHI and SalI sites with an enterokinase (EK) cleavage site (DDDDK) at the 5′-end of the coding region for the removal of the carrier. pET-28a-navidefensin2-2 was transformed into *E. coli* BL21(DE3)plysS for protein expression.

2.4. Expression, in vitro folding and identification of navidefensin2-2

Methods for expression, *in vitro* folding and purification of recombinant navidefensin2-2 are the same as those for AdDLP [5]. Briefly, we firstly collected the inclusion body and resuspended it in solubilization buffer. Refolding was performed by a linear urea gradient and the refolded fusion protein was digested by enterokinase (EK) (SinoBio, Shanghai) at room temperature for 2–3 h. Recombinant products were finally collected by RP-HPLC and its molecular weight (MW) was determined by MALDI-TOF mass spectra on a Kratos PC Axima CFR plus (Shimadzu Co. Ltd., Kyoto).

2.5. Chemical synthesis of peptides

Peptides corresponding to the α-helical region (named 2-1/2-2(helix)) and the γ-core (named 2-1/2-2(γ-core)) of navidefensin2-2 were synthesized by Xi'an Huachen Bio-Technology Co., Ltd. (Xian, China) and their purity was confirmed by RP-HPLC and MALDI-TOF (Table 1) (*Note*: naming of 2-1/2-2 is due to sequence identity in these two regions of navidefensin2-1 and 2-2).

2.6. Antimicrobial assays

Antibacterial assays were carried out according to the literature [27]. Briefly, overnight bacterial culture from a single colony was inoculated into fresh Luria broth (LB) and grew to late log-phase. A 10 μl aliquot of each of the cultures was diluted in 6 ml pre-heated LB containing 0.8% agar. The mixture was spread on a 9-cm Petri dish, giving a depth of 1 mm. After settling, 3-mm wells were punched in the plate and then peptide samples of different concentrations were added to each well. The agar plates were incubated overnight. Lethal concentration (C_L) values are calculated from a plot of d^2 against log n, where d is the diameter (in cm) and n is the amount of sample applied in the well (in nmol). The plot is linear and thus C_L can be calculated from the slope (k) and the intercept (m) of this plot. The formula used here is $C_L = 2.93/ak10^{m/k}$, where a is the thickness of the bacterial plate and C_L is in μM.

Microorganisms used in this study include: Gram$^+$ bacteria (*Micrococcus luteus* CGMCC 1.0290, *Bacillus megaterium* CGMCC 1.0459, *Bacillus subtilis* and *Bacillus sp.* DM-1); Gram$^-$ bacteria (*E. coli* ATCC25922 and *Salmonella typhimurium*); Fungus (*Beauveria* sp.); and Yeast (*Saccharomyces cerevisiae*). Sources of these microorganisms were listed in Table S2.

2.7. CD spectroscopy

CD spectra of navidefensin2-2 and 2-1/2-2(γ-core) were recorded on a JASCO J-720 spectropolarimeter (Jasco, Tokyo, Japan) at a protein concentration of 0.3 mg/ml dissolved in 5 mM sodium phosphate buffer (PB, pH 7.0) or in 50% trifluoroethanol (TFE) in PB. Data are expressed as mean residue molar ellipticity ([θ]). Percentages of peptide secondary structure elements were calculated with DICHROWEB from CD data (http://dichroweb.cryst.bbk.ac.uk).

2.8. Bioinformatics

Computational promoter analysis: Potential transcription factor (TF) binding sites in regulation regions of navidefensin promoters

Table 1
Synthetic peptides derived from navidefensin2-1/2-2.

Name	Region	Sequence	MW (Da)
2-1/2-2(helix)	19–30	ACAVRCLAQRRK-NH_2	1374.6 (1373.69)
2-1/2-2(γ-core)	31–42	GGKCKNGDCVCR-NH_2	1237.5 (1238.45)

Note: Numbers in the parentheses represent theoretical MWs.

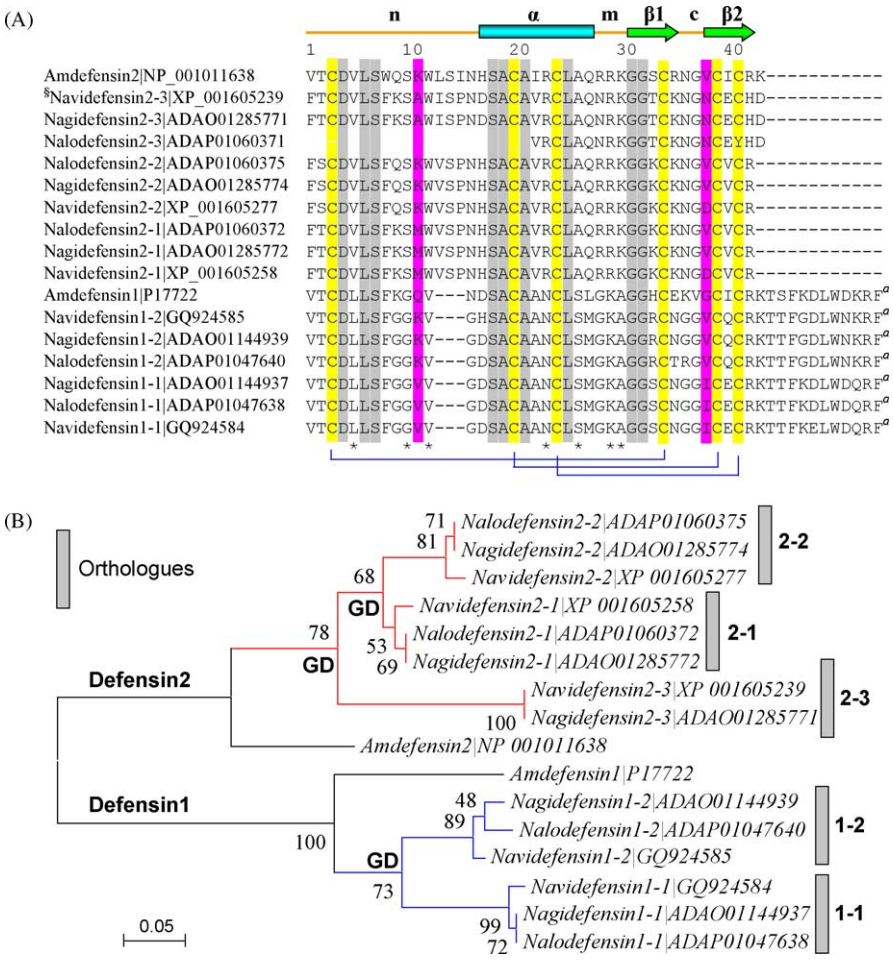

Fig. 1. The *Nasonia* defensins. (A) Multiple sequence alignment. §A predicted serine at site 20 from the genomic DNA of navidefensin2-3 is revised by a cysteine based on the conserved cystine framework in insect defensins. Cysteines are shadowed in yellow and other identical residues in grey. Cylinder and arrow respectively represent α-helix and β-strand, which are extracted from the model structure of navidefensin2-2. n, m and c represent three loop regions of the defensin family. Disulfide bridges are indicated by blue lines. [a]C-terminal amidation; *subtype-specific residues. (B) An unrooted neighbor-joining distance tree constructed from the alignment of amino acid sequences presented in (A) with Poisson correction for all sites under pairwise deletion. Numbers on interior branches represent bootstrap values. GD: gene duplication. (For interpretation of the references to color in this figure legend, the reader is referred to the web version of the article.)

were searched using the AliBaba2.1 program against the TRANSFAC database (http://www.gene-regulation.com/).

Structural modeling: The experimental structure of sapecin (PDB entry 1L4V) was selected as a template for modeling the navidefensin2-2 structure by SWISS-MODEL, a fully automated protein structure homology-modeling server (http://swissmodel.expasy.org/). Model quality was evaluated by Anolea and Verify3D. The 3D protein model of navidefensin2-2 has been deposited in the Protein Model database (http://www.caspur.it/PMDB/) under the id number of PM0076043.

Maximum likelihood analysis: Nucleotide sequences of 14 *Nasonia* defensins were aligned according to their amino acid alignment in Fig. 1A, and sites containing gaps were excluded in this analysis. An neighbor-joining tree constructed by MEGA 3.1 (http://www.megasoftware.net) was used for further statistical analysis. Codon-substitution models were selected to estimate the nonsynonymous-to-synonymous rate ratio ($\omega = dN/dS$) using the CODEML program of the PAML software package (http://abacus.gene.ucl.ac.uk/software/paml.html). Four models make two likelihood ratio tests (LRTs) by M0/M3 and M7/M8 [28]. M0 (one-ratio) assumes that all sites have the same ω ratio. M3 (discrete) uses a general discrete distribution with three site classes, with the proportions $p0$, $p1$, and $p2$ and the ω ratios $\omega 0$, $\omega 1$, and $\omega 2$. M7 (beta) allows sites to have 10 different x ratios in the interval (0, 1), which are calculated from the beta distribution with parameters p and q. M8 (beta and ω) adds an extra class of sites to the beta (M7) model and allows the sites to have $\omega > 1$. Upon detection of the positively selected signals, the calculation of posterior probabilities was completed using empirical Bayes method.

3. Results

3.1. The Nasonia defensins

Defensins are a group of evolutionarily related AMPs with conservation across almost the entire insect lineage. The hymenopteran insect *A. mellifera* genome encodes two defensin genes: defensin1 (also named royalisin) [23], which is a hymenoptera-specific AMP with a C-terminal extension of 11 residues and active on Gram$^+$ bacteria at low concentrations; defensin2 is a new defensin isoform with sequence and n-loop size similar to those from a diverse insect orders (e.g. coleoptera, phthiraptera and hemiptera). Defensin2 has not been identified regarding its biochemical function [29].

Nasonia is an emerging model parasitic insect genus which diverged approximately 120 million years ago from *A. mellifera*. From the genome sequences of three *Nasonia* species (*N. vitripennis*,

N. giraulti and *N. longicornis*), we identified a total of 15 defensins by computational prediction, all sharing high sequence similarity to two *A. mellifera* defensins (Fig. 1A). In comparison with the *A. mellifera* defensins, *defensin1* and *defensin2* have undergone independent gene duplication to create a mutigene family of five members (named 1-1, 1-2, 2-1, 2-2 and 2-3) in the *Nasonia* lineage. This lineage-specific duplication was further verified by phylogenetic analysis of all known hymenopteran defensins, in which members belonging to the *Nasonia defensin1* and *defensin2* respectively cluster together (Fig. S1, provided as Supplementary material). With the exception of nalodefensin2-3 from *N. longicornis*, all other *Nasonia* defensins have complete precursor organization comprising an N-terminal signal peptide, an acidic propeptide and a C-terminal mature defensin, in which dibasic residues as a typical processing signal are located between the propeptide and the mature peptide. Nalodefensin2-3 is an incomplete defensin because its genomic sequence is not available at present. Defensin1-1, 2-1, 2-2 and 2-3 between *N. giraulti* and *N. longicornis* possess identical mature peptide sequence.

The multiple sequence alignment in Fig. 1A highlights 15 residues (D^4, L^6, S^7, S^{18}, A^{19}, A^{21}, L^{25}, G^{31}, G^{32} and six cysteines, numbered according to navidefensin2-2) whose conservation is across the *Nasonia* lineage, where the cysteines are presumably involved in the formation of three disulfide bridges. A neighbor-joining distance tree divides the *Nasonia* defensins into two distinct subtypes with high bootstraps (78% and 100%, respectively), which respectively corresponds to *A. mellifera* defensin1 and 2 (Fig. 1B), indicating that each subtype forms a well-supported monophyletic clade. For each defensin member, an orthologous relationship among three species was clearly resolved in the tree, suggesting that such duplications occurred in the common ancestor of these three sibling species. Several subtype-specific residues were also identified at sites 5(V/L), 10(S/G), 12(W/V), 16(N/G), 23(R/N), 26(A/S), 29(R/K), 30(K/A), which could be relevant to functional divergence, if any, between the two subtypes.

3.2. Adaptive evolution of the Nasonia defensin family

To investigate whether positive selection has prompted accelerated evolution of the *Nasonia* defensin after gene duplication, we employed codon-substitution models to estimate the ratio of nonsynonymous-to-synonymous substitution ($dN/dS = \omega$) [28] (Table 2). The average ω ratio is 0.08 under the model M0, suggesting that a nonsynonymous mutation has only 8% as much chance as a synonymous mutation of being fixed and thus indicating that strong purifying selection, as a major force, drives the evolution of the *Nasonia* defensin. Two models (M3 and M8) detected a small proportion of sites (0.07–0.08) under positive selection with $\omega = 1.32–1.34$. Although only M3 was statistically supported by the likelihood ratio test (LRT) ($P < 0.01$) when compared with the control model M0, these two models convergently identified two sites (Lys^{11} and Asp^{35}, numbered according to navidefensin2-2) (Fig. 1A) suffering weak positive selection, which are respectively located in the n-loop preceding the conserved CSαβ-motif and the γ-core region. Positive selection was also observed in other defensins derived from mammals (e.g. α- and β-defensins [30,31]) and ants. In the ant defensin, two sites were detected as being positively selected [32] and one of them was also found in the n-loop despite not sharing an identical position to that of the parasitiod defensin. Given the N-terminal loop has been suggested to be involved in the modulation of the activity of insect defensins [20], positive selection at this region could represent adaptively convergent evolution between parasitiods and ants. In this work we have confirmed that the γ-core region is a key functional region of navidefensin2-2 (see below). These studies indicate that the immune systems of the social insect groups and parasitoids in hymenoptera may have responded similarly to the selection pressure caused by microbial pathogens and that the accelerated substitutions at the functional sites may be a consequence of adaptation to pathogens in a host-pathogen arms race.

3.3. Development-stage-specific expression of navidefensins

To study the development stage-specific expression of *Nasonia* defensins, we designed five specific PCR primers to amplify cDNAs prepared from the adults of *N. vitripennis* and *M. domestica* pupae infected by *N. vitripennis*. We found that only navidefensin1-1 and 1-2 were detected in the adult stage (Fig. 2A and B). In the infected pupa stage of the host, the expression of all defensin genes appeared to be shut off or at least were expressed at low level that was beyond our detection ability. Such expression pattern was also observed in the *Drosophila* antifungal peptide-drosomycin family, in which RT-PCR failed to detect the expression of all drosomycin isoforms in the *Drosophila* egg stage [33].

To provide regulatory information at the DNA level to explain which *cis*-regulatory elements could be responsible for the differential expression pattern between two subtypes of defensins in the adult stage, we performed comparative promoter analysis of about 1000 bp of promoter regions located in the upstream of a putative transcriptional start site (TSS). Conserved transcriptional factor (TF) binding motifs with a similar location within each subtype were defined by the AliBaba2.1 program, a specific tool for predicting TF sites by constructing specific matrices for each sequence analyzed instead of using predefined matrices for an unknown sequence [34]. As shown in Fig. 2C, all *Nasonia* defensin genes contain a core promoter comprising a potential eukaryotic initiator element matching the consensus [(TC)CA^{+1}N(TA)(TC)(TC)(TC)] (where A^{+1} is the base at which transcription starts, N is any of the four bases) and a TATA box located in an ideal distance [35]. The distal promoters of these defensins contain four motifs for CCAAT/enhancer binding protein-α (C/EBPα). The difference is within the proximal

Table 2
Maximum likelihood estimates of parameters and sites inferred to be under positive selection for the *Nasonia* defensin family.

Model	p	l	κ	Estimates of parameters	Positively selected sites
M0 (one-ratio)	1	−535.80	1.79	$\omega = 0.08$	None
M3 (discrete)	5	−518.34	1.45	$p0 = 0.31$, $\omega = 0$ $p1 = 0.61$, $\omega = 0.06$ $p2 = 0.08$, $\omega = 1.32$	11K**, 35D**
M7 (beta)	2	−521.89	1.40	$p = 0.22$, $q = 1.69$	Not allowed
M8 (beta and ω)	4	−519.62	1.45	$p0 = 0.93$, $p = 0.68$, $q = 14.14$ ($p1 = 0.07$), $\omega = 1.34$	11K**, 35D*

Note: p is the number of parameters in the ω distribution; l is the log likelihood; κ is transition/transversion rate ratio. Twice the log likelihood difference ($2\Delta l$) between null models (M0 and M7) and their alternative models (M3 and M8): M0/M3 = 34.92 (χ^2 significant value: $P < 0.01$); M7/M8 = 4.54 ($0.05 < P < 0.1$). Positively selected sites identified by the Bayes empirical Bayes (BEB) method under M3 and M8 with posterior probabilities (p) ≥ 0.95 and those with $p \geq 0.99$ are indicated by * and **.

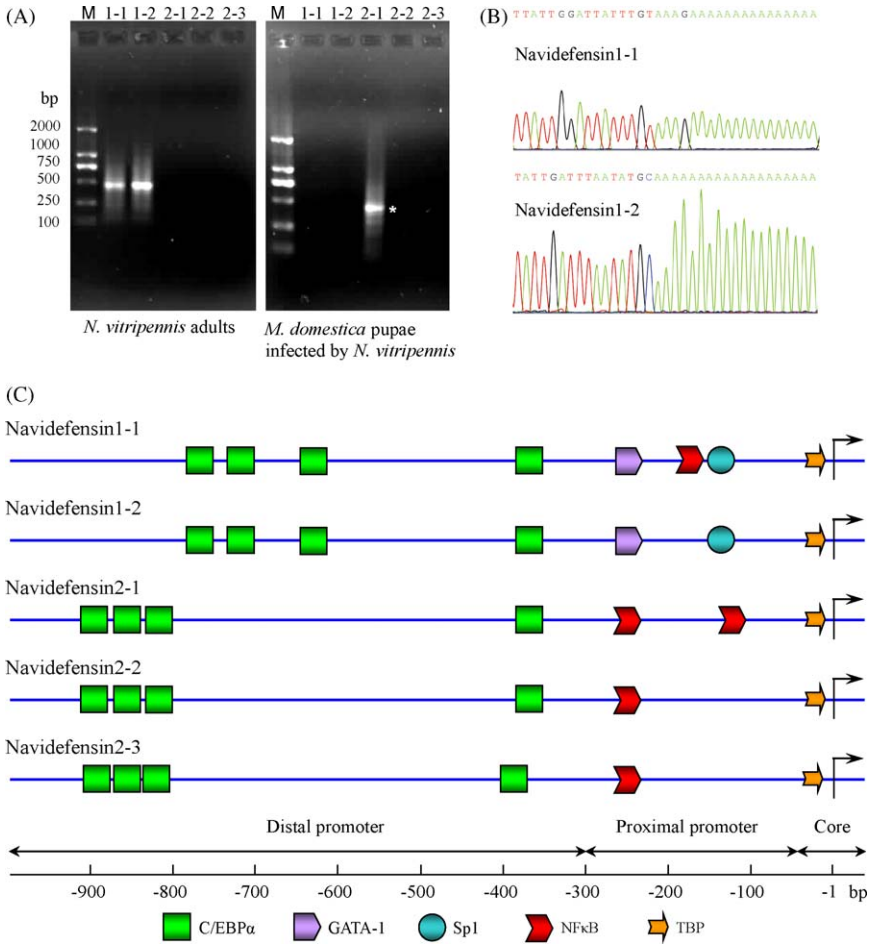

Fig. 2. Expression profiles and computational promoter analysis. (A) Detection of expression profiles of defensin genes in different developmental stages of *N. vitripennis* by RT-PCR. *Non-specific amplification from the *N. vitripennis* cuticular protein-like cDNA verified by DNA sequencing (GenBank accession no.: GU205189). (B) Sequencing maps showing partial 3′UTRs and poly(A) tails of navidefensin1-1 and 1-2. (C) Schematic structure of navidefensin promoters. Arrows represent potential transcription start sites. For the detailed location of TF binding sites at the nucleotide level, see Fig. S2.

promoter, in which all the navidefensin genes contain at least one nuclear factor kB (NFkB) response element with the exception of navidefensin1-2. NFkB is an evolutionarily conserved mediator of immune and inflammatory responses and affects the various cells involved in immune response. The presence of the NFkB response elements in the promoters of these defensins suggests a putative inducible expression feature of these genes [36]. Compared with the defensin2 subtype, defensin1 genes have two extra TF binding motifs in the proximal promoter, one for specificity protein1 (SP1) and another for GATA-1. It is known that adjacent GATA and kB-like motifs can regulate the expression of the *Drosophila* antimicrobial peptide – Cecropin A1 [37]. Whether these two specific TF motifs work as *cis*-regulatory elements to regulate the constitutive expression of the subtype 1 genes in the adult stage remains an open question.

3.4. Recombinant production and characterization of navidefensin2-2

Navidefensin2-2 was chosen for recombinant expression because it represents a subtype of hymenopteran defensins whose members' biochemical function is unknown at present. In order to improve the expression of navidefensin2-2 in *E. coli*, we optimized its encoding region sequence by replacing 6 rare codons that are infrequently used by *E. coli* with normal codons (Fig. 3A), a strategy successfully used in the expression of recombinant hymenoptaecin-like domain (HLD) from *N. vitripennis* [38]. The synthetic gene was ligated into pET-28a vector (Fig. 3B). The His-tagged fusion protein was expressed in an insoluble inclusion body form in *E. coli* BL21 (DE3) plysS cells, and thus refolding was carried out according to the method previously used in AdDLP [5]. Imidazole of the eluate was removed by RP-HPLC (Fig. 3C), in which one major peak eluted at the retention time (RT) of 20 min exhibited a strong antibacterial activity against the Gram$^+$ *B. megaterium* (Fig. 3D) and was thus collected for EK digestion. The digested product was further purified by RP-HPLC (Fig. 4A), of which the 21 min peak represents an antibacterial component (Fig. 4B) and thus collected for MALDI-TOF to determine its MW. The MW is 4639.8 Da (Fig. 4C) and perfectly matches the theoretical value of navidefensin2-2 (4640.40 Da). The final yield of the recombinant navidefensin2-2 is about 1 mg/l *E. coli* culture.

3.5. Structural feature of navidefensin2-2

We evaluated the secondary structure feature of recombinant navidefensin2-2 by CD analysis. As shown in Fig. 5A, the CD spectrum of navidefensin2-2, measured in 5 mM phosphate buffer, had a negative minimum at 204 nm, similar to that of the recombinant Lqh3, a scorpion toxin adopting the CSαβ folding [39]. The quality of this spectrum is appropriate for calculating the secondary structure content because it is nearly identical with the calculated spectrum by CDSSTR method and reference data set 4. Based on the CD data, we estimated secondary structures in

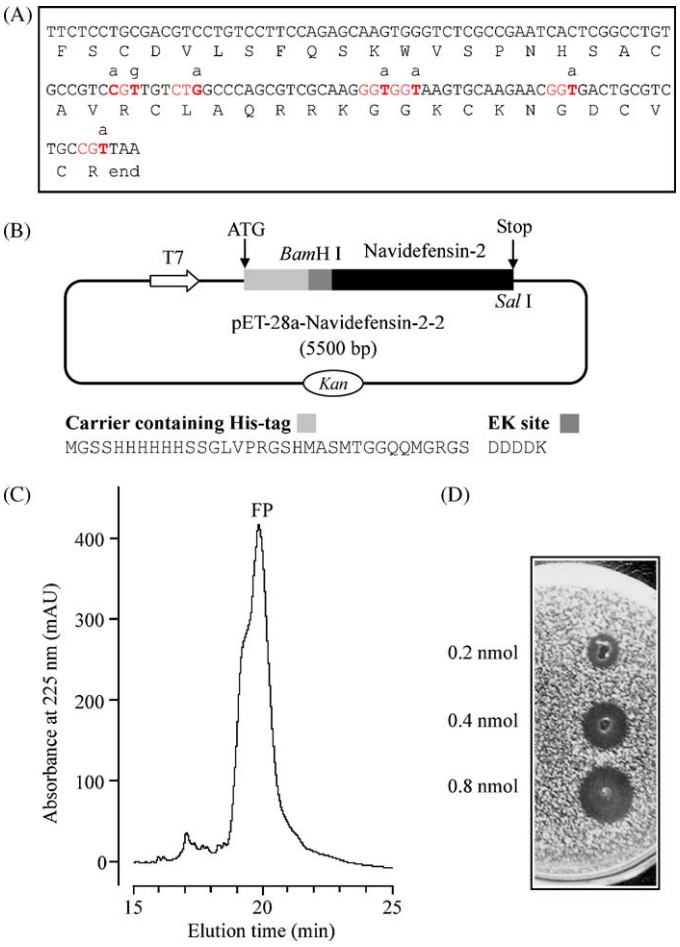

Fig. 3. Expression and purification of the fusion protein. (A) Optimization of the coding region of navidefensin to remove rare codons in *E. coli*. Optimized codons are highlighted in red and substitution bases boldfaced. (B) Construction of pET-28a-navidefensin2-2 expression vector. The synthesized DNA sequence was inserted into BamHI and SalI sites of pET-28a with an EK cleavage site at the 5′ end. (C) RP-HPLC showing the purified fusion protein (FP). C18 column was equilibrated with 0.1% TFA and the purified proteins were eluted from the column with a linear gradient from 0 to 60% acetonitrile in 0.1% TFA within 40 min. (D) Concentration-dependent antibacterial activity of the fusion protein against *B. megaterium*. (For interpretation of the references to color in this figure legend, the reader is referred to the web version of the article.)

navidefensin2-2 by DICHROWEB. The results indicate that the recombinant peptide contains 18% α-helix and 24% β-sheet, compatible with some structurally known defensins and scorpion toxins (e.g. defensin A (pdb entry 1ICA) and charybdotoxin (pdb entry 2CRD)).

To obtain a reliable structure model with compatible secondary structure contents with the CD results, we applied comparative modeling to construct the structure of navidefensin2-2. As expected, BLAST search identified two structurally known insect defensins (defensin A and sapecin) as the closest homologues with about 50% sequence identity. In addition to six cysteines, some residues associated with the formation of the structural core are also conserved between navidefensin2-2 and these two defensins (data not shown). The conservation thus supports rationality for computational prediction of the navidefensin2-2 structure. When the experimental structure of sapecin was used as a template, we obtained a structure of navidefensin2-2 which has a similar secondary structure content with the CD data. In this model, the α-helical region spans the sequence ^{17}HSACAVRCLAQ^{27} and the two β-strands include ^{31}GGKCK^{35} and ^{38}DCVCR^{42} (Fig. 5B). Three conserved disulfide bridges are also predicted in navidefensin2-2. Overall, the CSαβ core region exhibits more positively charged surface while the n-loop is more neutral and negative (Fig. 5C).

3.6. Antibacterial activity of navidefensin2-2 and its putative functional site

We assessed antimicrobial activity of recombinant navidefensin2-2 against several microorganisms and found that this peptide only inhibited the growth of two Gram$^+$ bacteria (*M. luteus* and *B. megaterium*) at micromolar concentrations (Table 3). Under the same condition, navidefensin2-2 exhibited no effect on two Gram$^-$ bacteria (*E. coli* and *S. typhimurium*), two additional Gram$^+$ bacteria (*B. subtilis* and *Bacillus* sp. DM-1), and the fungus *Beauveria sp.* and the yeast *S. cerevisiae*. *B. megaterium* is the most sensitive species to navidefensin2-2 with a lethal concentration of 1.5 μM. A similar anti-*B. megaterium* activity was also found in the fusion protein, indicating that the amino-terminal extension of navidefensin2-2 did not affect its antibacterial function. This is further strengthened by the observation that the carrier itself had no effect on *B. megaterium*.

To obtain information regarding the functional site of navidefensin2-2, we evaluated antibacterial activity of two synthetic peptides derived from navidefensin2-2, one corresponding to the helical region (named 2-1/2-2(helix)) and another to the γ-core region (named 2-1/2-2(γ-core)), which both display positively charged molecular surfaces (data not shown). The results indicated that 2-1/2-2(helix) lacked detectable activity against all the microbial strains listed in Section 2 when the pure peptide (1.6 nmol) was tested. On the contrary, 2-1/2-2(γ-core) exhibited a broader antimicrobial spectrum than the intact molecule, which inhibited all four Gram$^+$ bacteria and the fungus and the yeast but no effect was observed on the two Gram$^-$ bacteria. Although the potency of 2-1/2-2(γ-core) for the same sensitive bacteria was lower than the intact peptide, this active peptide only corresponds a small fragment and thus represents a major active site of navidefensin2-2. Activity against more Gram$^+$ bacteria, the fungus and the yeast by 2-1/2-2(γ-core) suggests that other regions of this defensin could participate in determination of microbial specificity.

3.7. 2-1/2-2(γ-Core) is a β-sheet peptide structurally similar to naturally occurring AMPs

To understand the structural basis of the active γ-core, we analyzed its structural feature by CD analysis. As shown in Fig. 6,

Table 3
Lethal concentrations (μM) of navidefensin2-2 and its truncated peptides.

	FP	Navidefensin2-2	2-1/2-2(helix)	2-1/2-2(γ-core)
Gram$^+$ bacteria				
M. leutues	N.D	4.54	N.A	25.98
B. megaterium	2.3	1.5	N.A	8.93
B. subtilis	N.D	N.A	N.A	10.77
Bacillus sp. DM-1	N.D	N.A	N.A	33.80
Gram$^-$ bacteria				
E. coli	N.D	N.A	N.A	N.A
S. typhimurium	N.D	N.A	N.A	N.A
Fungus				
Beauveria sp.	N.D	N.A	N.A	17.68
Yeast				
S. cerevisiae	N.D	N.A	N.A	52.01

Note: N.D: not determined; N.A: no activity, indicating that no inhibition zone was observed at 1.6 nmol peptide/well; FP: fusion protein. The assays were performed in duplicate in one experiment.

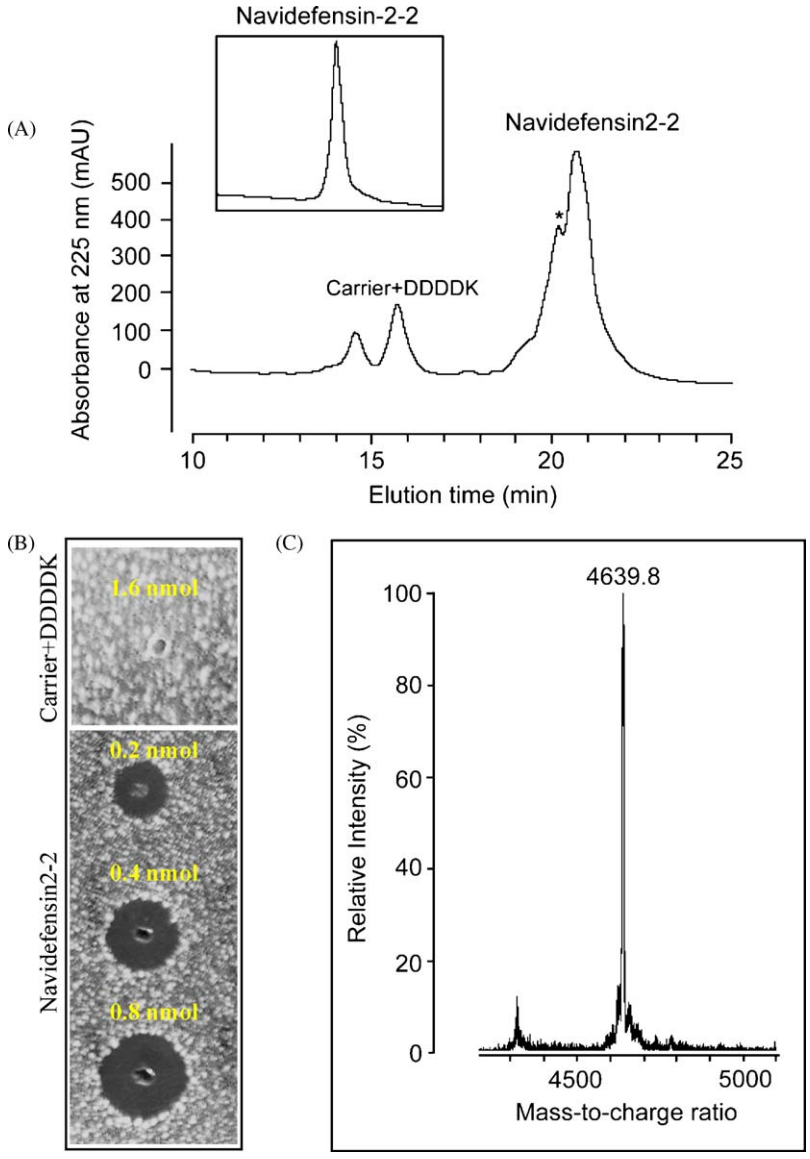

Fig. 4. Purification and characterization of recombinant navidefensin2-2. (A) RP-HPLC showing the EK-digested product under the same condition in Fig. 3C. *Undigested fusion protein; inset represents the purified peptide. (B) Inhibition zones of different concentrations of peptides against *B. megaterium*. (C) Determination of the MW of navidefensin2-2 by MALDI-TOF.

the CD spectra of 2-1/2-2(γ-core), measured in 5 mM phosphate buffer and in the presence of 50% TFE, displayed a similar ellipticity between 190 and 240 nm, as identified by a negative band around 210 nm without a band at 222 nm. These data indicate that this peptide mainly adopts a rigid β-sheet structure (39% in the phosphate buffer and 42% in TFE), resembling the secondary structure corresponding to the region in navidefensin2-2.

Such a structural feature is commonly possessed by several naturally occurring AMPs, such as protegrin1, a cysteine-rich β-sheet peptide isolated from porcine leukocytes, and gomesin, a cysteine-rich small AMP from the spider hemocytes (Fig. 7A). Structurally, these two AMPs can be well superimposed with the 2-1/2-2(γ-core) structure derived from the intact molecule (Fig. 7B). More importantly, an amphipathic design essential for antibacterial activity of the most AMPs also exists in the structure of 2-1/2-2(γ-core) where three hydrophobic residues (Cys^{39}, Val^{40}, and Cys^{41}) and three cationic residues (Lys^{33}, Lys^{35} and Arg^{42}) are separately clustered into distinct domains in its molecular surface (Fig. 7C).

4. Discussion

Nasonia is an emerging model insect whose genome sequences provide a new resource for the discovery of genes involved in innate immunity of parasitic insects (Tian and Zhu, unpublished data). So far, only one known *Nasonia* AMP is nahymenoptaecin-1 which is an orthologoue of bee hymenoptaecin in *N. vitripennis* [38]. The work presented here provides the second example of *Nasonia* AMPs, in which a conserved defensin gene family was identified in three sibling species of *Nasonia*. In comparison with *A. mellifera*, *Nasonia* immune genes appear to have evolved a more complicated precursor organization through exon-shuffling (i.e. nahymenoptaecin-1) or more numbers by gene duplication followed by positive selection in the active site (i.e. defensins). Biological significance of such immune diversification between parasitic and non-parasitic insects awaits further investigation. Successful expression of navidefensin2-2 undoubtedly paves the way to these related studies.

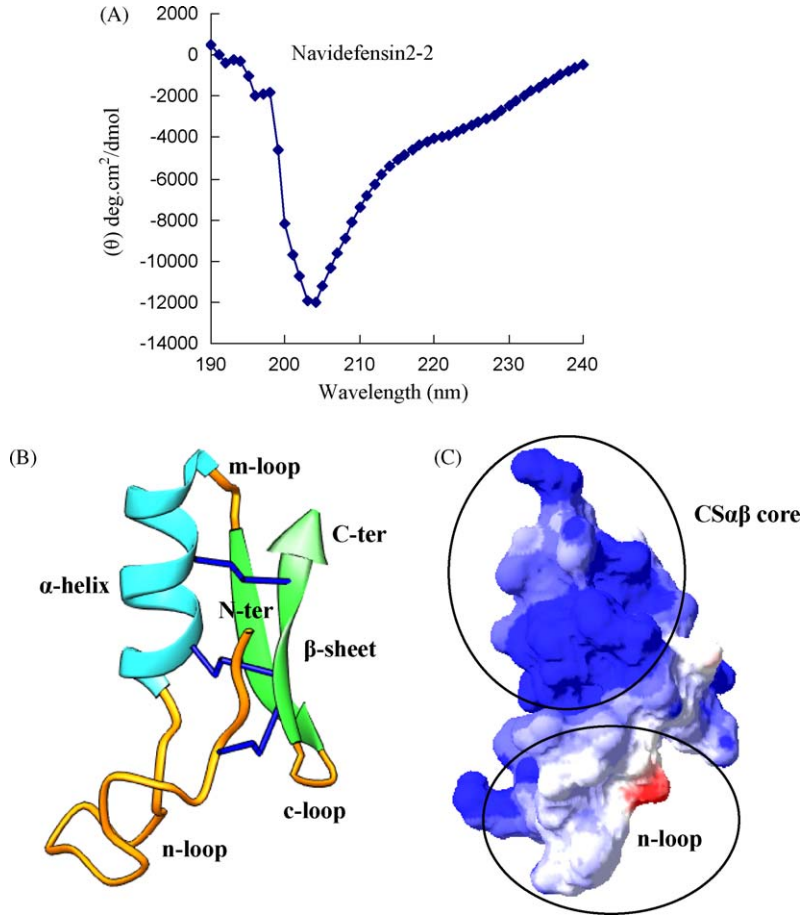

Fig. 5. Structural feature of navidefensin2-2. (A) CD spectra of navidefensin2-2 in PB buffer and (B) the model structure of navidefensin2-2. Ribbon showing global fold, in which disulfide bridges are indicated by blue sticks. (C) Electrostatic potential map. Positive and negative charges are shown in red and blue, respectively. (For interpretation of the references to color in this figure legend, the reader is referred to the web version of the article.)

Since the first active fragment was characterized in the insect defensin sapecin B [40], several other peptide fragments have also been found in several insect defensins, such as tenecin-1 [41], ordefensin [42], adefensin [43], coprisin [44], protaetiamycin [45] (Fig. 8). Due to overall negatively charged feature, two n-loop-derived peptides have been verified inactive. However, cationic alpha-helix- or γ-core-derived peptides exhibited some contradictory results. For example, peptides derived from the helical regions of five insect defensins (sapecin B, coprisin, protaetiamycin, adefensin and ordefensin) displayed clear antimicrobial activity whereas helix-derived peptides were found inactive in tenecin-1 and navidefensin2-2. Alternatively, in the latter case the active site is located in the γ-core. The absence of activity in the helical regions of tenecin-1 and navidefensin2-2 could be explained by an amino acid substitution at site 27 where it is either a cationic residue (Arg^{27}) or a polar side-chain (Gln^{27}). By contrast, a hydrophobic residue (Leu or Ile) occupies this position in other active helix-derived peptides from coprisin, protaetiamycin, adefensin and ordefensin. Such substitution may disrupt the hydrophobic and hydrophilic balance and thus leads to the loss of antimicrobial activity. Yamada and Natori found that two regions corresponding to the γ-core of sapecin B were inactive, however, in their study the γ-core was seperated into two smaller fragments which may hamper the formation of a β-sheet. Thus the functional significance of the γ-core of sapecin B needs to be re-evaluated in the future.

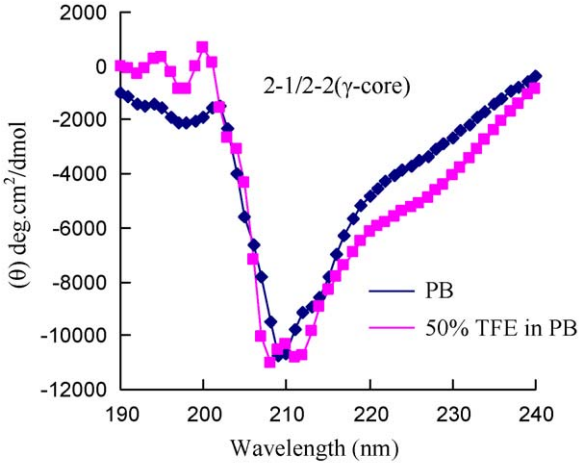

SS (%)	α-helix	β-sheet	Others
PB	7	39	53
50% TFE in PB	10	42	47

Fig. 6. CD spectra of 2-1/2-2(γ-core) in PB buffer and 50% TFE.

An interesting observation emerging from the above studies is that all active peptides derived from insect defensins exhibit a broader antimicrobial spectrum than their intact parent molecule [36–41]. In this case, more microbial strains resistant to intact defensins become sensitive to truncated peptides. These findings could be of biological significance if we consider the degradation process of proteins in live organisms. It is likely that degradation of

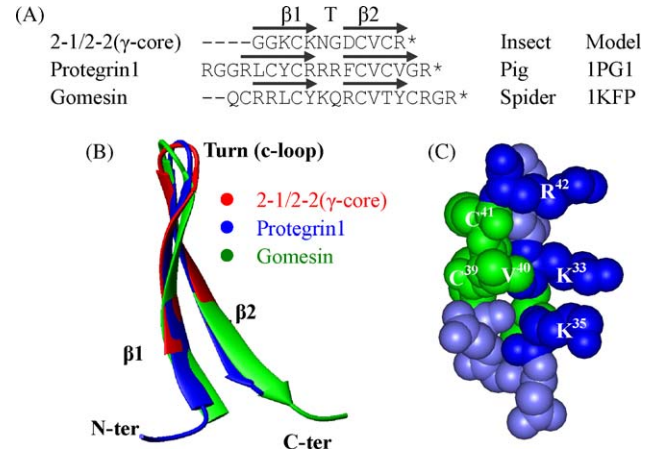

Fig. 7. Structural feature of active site of navidefensin2-2. (A) Comparison of 2-1/2-2(γ-core) with two antimicrobial peptides with similar structural conformation. *C-terminal amidation. T: turn. (B) Structural superimposition and (C) clustering of positively charged (blue) and hydrophobic residues (green) into two distinct domains in 2-1/2-2(γ-core). Polar or negatively charged residues are highlighted in bright blue. (For interpretation of the references to color in this figure legend, the reader is referred to the web version of the article.)

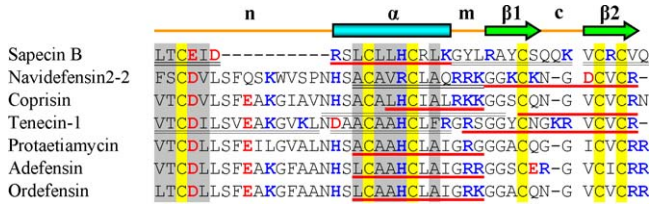

Fig. 8. Sequence alignment of several CITDs with their functional regions characterized. Antibacterial regions are underlined once in red and non-functional regions underlined twice. (For interpretation of the references to color in this figure legend, the reader is referred to the web version of the article.)

a defensin into active fragments represents a defense strategy of insect innate immunity when infection occurs. Isolation and characterization of such fragments from infected tissues will provide evidence in favor of this hypothesis.

Acknowledgements

This work was supported by the National Natural Science Foundation of China (30730015, 90608009 and 30621003) and the 973 Program from the Ministry of Science and Technology of China (2010CB945304).

Appendix A. Supplementary data

Supplementary data associated with this article can be found, in the online version, at doi:10.1016/j.dci.2010.01.012.

References

[1] Dimarcq JL, Bulet P, Hetru C, Hoffmann J. Cysteine-rich antimicrobial peptides in invertebrates. Biopolymers 1998;47:465–77.
[2] Bulet P, Stöcklin R, Menin L. Anti-microbial peptides: from invertebrates to vertebrates. Immunol Rev 2004;198:169–84.
[3] Zhu S, Gao B, Tytgat J. Phylogenetic distribution, functional epitopes and evolution of the CSαβ superfamily. Cell Mol Life Sci 2005;62:2257–69.
[4] Cornet B, Bonmatin JM, Hetru C, Hoffmann JA, Ptak M, Vovelle F. Refined three-dimensional solution structure of insect defensin A. Structure 1995;3:435–48.
[5] Gao B, Rodriguez Mdel C, Lanz-Mendoza H, Zhu S. AdDLP, a bacterial defensin-like peptide, exhibits anti-*Plasmodium* activity. Biochem Biophys Res Commun 2009;387:393–8.
[6] Yount NY, Yeaman MR. Multidimensional signatures in antimicrobial peptides. Proc Natl Acad Sci USA 2004;101:7363–8.
[7] Yeaman MR, Yount NY. Unifying themes in host defence effector polypeptides. Nat Rev Microbiol 2007;5:727–40.
[8] Dassanayake RS, Silva Gunawardene YI, Tobe SS. Evolutionary selective trends of insect/mosquito antimicrobial defensin peptides containing cysteine-stabilized alpha/beta motifs. Peptides 2007;28:62–75.
[9] Bulet P, Cociancich S, Reuland M, Sauber F, Bischoff R, Hegy G, et al. A novel insect defensin mediates the inducible antibacterial activity in larvae of the dragonfly *Aeschna cyanea* (Paleoptera, Odonata). Eur J Biochem 1992;209:977–84.
[10] Cociancich S, Goyffon M, Bontems F, Bulet P, Bouet F, Menez A, et al. Purification and characterization of a scorpion defensin, a 4 kDa antibacterial peptide presenting structural similarities with insect defensins and scorpion toxins. Biochem Biophys Res Commun 1993;194:17–22.
[11] Charlet M, Chernysh S, Philippe H, Hetru C, Hoffmann JA, Bulet P. Innate immunity. Isolation of several cysteine-rich antimicrobial peptides from the blood of a mollusc, *Mytilus edulis*. J Biol Chem 1996;271:21808–13.
[12] Nakajima Y, van der Goes van Naters-Yasui A, Taylor D, Yamakawa M. Two isoforms of a member of the arthropod defensin family from the soft tick, *Ornithodoros moubata* (Acari: Argasidae). Insect Biochem Mol Biol 2001;31:747–51.
[13] Mygind PH, Fischer RL, Schnorr KM, Hansen MT, Sönksen CP, Ludvigsen S, et al. Plectasin is a peptide antibiotic with therapeutic potential from a saprophytic fungus. Nature 2005;437:975–80.
[14] Gueguen Y, Herpin A, Aumelas A, Garnier J, Fievet J, Escoubas JM, et al. Characterization of a defensin from the oyster *Crassostrea gigas*. Recombinant production, folding, solution structure, antimicrobial activities, and gene expression. J Biol Chem 2006;281:313–23.
[15] Zhu S. Discovery of six families of fungal defensin-like peptides provides insights into origin and evolution of the CSαβ defensins. Mol Immunol 2008;45:828–38.
[16] Zhu S, Tytgat J. The scorpine family of defensins: gene structure, alternative polyadenylation, and fold recognition. Cell Mol Life Sci 2004;61:1751–63.
[17] Gao B, Sherman P, Luo L, Bowie J, Zhu S. Structural and functional characterization of two genetically related meucin peptides highlights evolutionary divergence and convergence in antimicrobial peptides. FASEB J 2009;23:1230–45.
[18] Wachinger M, Kleinschmidt A, Winder D, von Pechmann N, Ludvigsen A, Neumann M, et al. Antimicrobial peptides mellitin and cecropin inhibit replication of human immunodeficiency virus 1 by suppressing viral gene expression. J Gen Virol 1998;79:731–40.
[19] Blandin S, Moita LF, Köcher T, Wilm M, Kafatos F, Levashina EA. Reverse genetics in the mosquito *Anopheles gambiae*: targeted disruption of the defensin gene. EMBO Rep 2002;3:852–6.
[20] Landon C, Barbault F, Legrain M, Guenneugues M, Vovelle F. Rational design of peptides active against the gram positive bacteria *Staphylococcus aureus*. Proteins 2008;72:229–39.
[21] Matsuyama K, Natori S. Purification of three antibacterial proteins from the culture medium of NIH-Sape-4, an embryonic cell line of *Sarcophaga peregrina*. J Biol Chem 1988;263:17112–6.
[22] Lambert J, Keppi E, Dimarcq JL, Wicker C, Reichhart JM, Dunbar B, et al. Insect immunity: isolation from immune blood of the dipteran *Phormia terranovae* of two insect antibacterial peptides with sequence homology to rabbit lung macrophage bactericidal peptides. Proc Natl Acad Sci USA 1989;86:262–6.
[23] Fujiwara S, Imai J, Fujiwara M, Yaeshima T, Kawashima T, Kobayashi K. A potent antibacterial protein in royal jelly. Purification and determination of the primary structure of royalisin. J Biol Chem 1990;265:11333–7.
[24] Volkoff AN, Rocher J, d'Alençon E, Bouton M, Landais I, Quesada-Moraga E, et al. Characterization and transcriptional profiles of three *Spodoptera frugiperda* genes encoding cysteine-rich peptides. A new class of defensin-like genes from lepidopteran insects? Gene 2003;319:43–53.
[25] Werren JH, Richards S, Desjardins CA, Niehuis O, Gadau J, Colbourne JK, et al. Functional and evolutionary insights from the genomes of three parasitoid *Nasonia species*. Science 2010;327:343–8.
[26] Zhu S, Gao B. Molecular characterization of a new scorpion venom lipolysis activating peptide: evidence for disulfide bridge-mediated functional switch of peptides. FEBS Lett 2006;580:6825–36.
[27] Hultmark D. Quantification of antimicrobial activity, using the inhibition-zone assay. In: Wiesner A, Dumphy AG, Marmaras VJ, Morishima I, Sugumaran M, Yamakawa M, editors. Techniques in insect immunology. SOS Publications Fair; 1998. p. 103–7.
[28] Yang Z, Nielsen R, Goldman N, Pedersen AM. Codon-substitution models for heterogeneous selection pressure at amino acid sites. Genetics 2000;431–49.
[29] Klaudiny J, Albert S, Bachanová K, Kopernický J, Simúth J. Two structurally different defensin genes, one of them encoding a novel defensin isoform, are expressed in honeybee *Apis mellifera*. Insect Biochem Mol Biol 2005;35:11–22.
[30] Lynn DJ, Lloyd AT, Fares MA, O'Farrelly C. Evidence of positively selected sites in mammalian alpha-defensins. Mol Biol Evol 2004;21:819–27.
[31] Morrison GM, Semple CA, Kilanowski FM, Hill RE, Dorin JR. Signal sequence conservation and mature peptide divergence within subgroups of the murine beta-defensin gene family. Mol Biol Evol 2003;20:460–70.
[32] Viljakainen L, Pamilo P. Selection on an antimicrobial peptide defensin in ants. J Mol Evol 2008;67:643–52.
[33] Tian C, Gao B, Rodriguez MC, Lanz-Mendoza H, Ma B, Zhu S. Gene expression, antiparasitic activity, and functional evolution of the drosomycin family. Mol Immunol 2008;453909–16.

[34] Grabe N. AliBaba2: context specific identification of transcription factor binding sites. In Silico Biol 2002;2:S1–5.
[35] Lodish H, Berk A, Zipursky SL, Matsudaira P, Baltimore D, Darnell J. Molecular cell biology. New York; 2000.
[36] Uvell H, Engström Y. A multilayered defense against infection: combinatorial control of insect immune genes. Trends Genet 2007;23:342–9.
[37] Kadalayil L, Petersen UM, Engström Y. Adjacent GATA and kappa B-like motifs regulate the expression of a *Drosophila* immune gene. Nucleic Acids Res 1997;25:1233–9.
[38] Gao B, Zhu S. Characterization of a hymenoptaecin-like antimicrobial peptide in the parasitic wasp *Nasonia vitripennis*. Process Biochem 2010;45:139–46.
[39] Karbat I, Kahn R, Cohen L, Ilan N, Gilles N, Corzo G, et al. The unique pharmacology of the scorpion alpha-like toxin Lqh3 is associated with its flexible C-tail. FEBS J 2007;274:1918–31.
[40] Yamada K, Natori S. Characterization of the antimicrobial peptide derived from sapecin B, an antibacterial protein of *Sarcophaga peregrina* (flesh fly). Biochem J 1994;298:623–8.
[41] Lee KH, Hong SY, Oh JE, Kwon M, Yoon JH, Lee J, et al. Identification and characterization of the antimicrobial peptide corresponding to C-terminal beta-sheet domain of tenecin 1, an antibacterial protein of larvae of *Tenebrio molitor*. Biochem J 1998;334:99–105.
[42] Ishibashi J, Saido-Sakanaka H, Yang J, Sagisaka A, Yamakawa M. Purification, cDNA cloning and modification of a defensin from the coconut rhinoceros beetle, *Oryctes rhinoceros*. Eur J Biochem 1999;266:616–23.
[43] Saido-Sakanaka H, Ishibashi J, Sagisaka A, Momotani E, Yamakawa M. Synthesis and characterization of bactericidal oligopeptides designed on the basis of an insect anti-bacterial peptide. Biochem J 1999;338: 29–33.
[44] Hwang JS, Lee J, Kim YJ, Bang HS, Yun EY, Kim SR, et al. Isolation and characterization of a defensin-like peptide (coprisin) from the dung beetle, *Copris tripartitus*. Intern J Pept 2009. doi: 10.1155/2009/136284.
[45] Shin S, Kim JK, Lee JY, Jung KW, Hwang JS, Lee J, et al. Design of potent 9-mer antimicrobial peptide analogs of protaetiamycine and investigation of mechanism of antimicrobial action. J Pept Sci 2009;15:559–68.